WAVELETS IN THE FREQUENCY DOMAIN FOR NARROWBAND PROCESS DETECTION

Peter Willett and Zhen Wang*

U-157, University of Connecticut
Storrs, CT 06269-3157
willett/wangz@engr.uconn.edu

Roy Streit

Naval Undersea Warfare Center
Newport, RI 02841
streitrl@npt.nuwc.navy.mil

ABSTRACT

Detecting signals that are long, weak, and narrowband is a well known and important problem in acoustic signal processing. In this paper an ad hoc scheme is developed: its stages include the DFT, a multiresolution decomposition in the frequency domain, and a GLRT. The computational load is light, and the performance is remarkably good. This is so not just in the original narrowband situation, but also, due to an inherent adaptivity to the data, in the detection of signals that are relatively broadband in nature. Generalizations are given to CFAR operation in both prewhitened and unwhitened cases, and to the detection of multi-band signals. As regards the last, it is discovered that there is little loss from over-estimating the number of bands.

1. INTRODUCTION

In this paper we are concerned with the detection of extremely weak and long-duration narrowband signals. Such signals can arise in a variety of applications, such as system-condition diagnosis (perhaps indicative of a problematic vibration), industrial process monitoring (perhaps chatter in grinding), astrophysics (pulsars, etc.) and underwater surveillance. At any rate, detecting them is important. Although various physics-based models are possible, we confine ourselves to the narrowband model, that the signal to be detected arises from the passage of a white Gaussian process through a narrowband filter. This band is not known, although it can be assumed not to vary with respect to time. Thus a detector "tuned" for a bandwidth of 10 Hz may perform poorly when in truth the bandwidth is 30Hz. Our goal is to establish a detection structure that can take advantage of a narrowband nature, yet is robust when the bandwidth increases.

*This research was supported by ONR through contracts N66604-99-1-5021 and N00014-98-1-0049.

2. DETECTION STRUCTURES

2.1. Modeling and Detector Background

The problem considered in this paper is of detection of a long-duration bandpass signal: its energy is known to be concentrated in contiguous frequencies. But since these frequencies are unknown, the hypotheses to be tested are composite. The magnitude-squared FFT is taken on the time-domain observations, and we proceed in the frequency domain. We write in a matrix a block of NL time domain observations as $\mathbf{x} = (\mathbf{x}_1, \mathbf{x}_2, ..., \mathbf{x}_L)$, where $\mathbf{x}_m$ is a column vector of dimension N whose k^{th} element is the time sample of index $(m-1)L+k$. Each column is immediately transformed to its magnitude-squared frequency domain equivalent $\mathbf{X}_m$, and recorded as $\mathbf{X} = (\mathbf{X}_1, \mathbf{X}_2, ..., \mathbf{X}_L)$. It is assumed that X_{jm}'s are independent.

The probability density function (pdf) of the j^{th} element of $\mathbf{X}_m, m = 1, 2, ..., L$, follows an exponential distribution with parameter β_j. More specifically, presented in a hypothesis testing framework, we have the model

$$\begin{aligned} \mathbf{H}_0 \quad &: \quad \beta_j = \mu_{0,0} = 1, \;\; 1 \le j \le N \\ \mathbf{H}_1 \quad &: \quad \beta_j = \begin{cases} \mu_{1,1} & k_1 \le j \le k_2 \\ 1, & \text{else} \end{cases} \end{aligned} \tag{1}$$

Signal energy is to be found in the (unknown) subset $\{k_1, k_1+1, ..., k_2\}$ and $\theta = \{\mu_{1,1}, k_1, k_2\}$ are the parameters.

In detection with unknown parameters, the GLRT approach replaces these by their maximum likelihood estimates (MLEs): $T_{GLR}(\mathbf{X}) = \frac{max_{\theta \in \Theta_1}\{f_\theta(\mathbf{X})\}}{f_{\theta_0}(\mathbf{X})}$, where the set Θ_1 includes all possible choices of parameter θ under H_1. Based on the model of (1), the GLRT amounts to enumerating all possible values when discrete parameterization is involved, and hence it is unappealing here.

Nuttall's power-law detector [1] has attracted considerable attention due to its simple implementation

and good performance. It is written as

$$T_{PL} = \sum_{m=1}^{L}\sum_{j=1}^{N} X_{jm}^{\nu} \quad (2)$$

where ν is a real exponent. New versions of the power-law detectors were developed in [3] to take advantage of a tendency for signals (actually transient signals in that paper) to agglomerate their energies in the transform domain. For instance, the detector combining 2 contiguous FFT bins is simply formed as

$$T_{f2} = \sum_{m=1}^{L-1}\sum_{j=1}^{N}(X_{j,m} + X_{j+1,m})^{\nu} \quad (3)$$

with a similar expression for T_{f3}. Constant false-alarm rate (CFAR) and self-whitening versions of these statistics have also been developed.

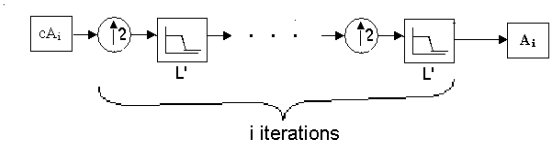

Fig. 1. Reconstructing the i^{th} level approximation A_i from cA_i. L' is the reconstruction low-pass filter.

2.2. The Detector

Due to the assumed frequency contiguity of signals of interest, the $\{\beta_j\}$'s are locally-smooth. This motivates us to estimate $\{\beta_j\}$'s using wavelet coefficients in the frequency domain. Here only the Haar wavelet [2] is used due to its easy implementation.

Assume the data has been preprocessed as in section 2.1. Detection proceeds as follows:

1. – Coarsely estimate the β's by averaging across time, as

$$\beta_j^{uML} = \frac{\sum_{m=1}^{L} X_{jm}}{L} \quad (4)$$

for $j = 1, 2, ..., N$, the superscript uML denotes unconstrained ML estimation.

2. – Do a multi-resolution decomposition on $\{\beta_j^{uML}\}$. With the vector $\{\beta_j^{uML}\}$ as the input signal, the wavelet decomposition process operates with successive approximations being decomposed in turn and generating lower resolution coefficients having only half the length due to downsampling. We denote the k^{th} element of the i^{th}-level approximation decomposition as $cA_i(k)$.

3. – Interpolate each scale level to the same length. The process, as in figure 1, yields a reconstructed approximation A_i having the same length N as the original signal, and presumably recognizable as an approximation of it.

4. – For each scale compute the mean level:

$$\eta_i = \frac{1}{N}\sum_{k=1}^{N} A_i(k) \quad (5)$$

5. – For each scale find the region of signal energy. It is assumed that if the bandwidth of the signal is such that its appearance will be most evident at scale i, then there will be a peak in $\{A_i(k)\}$ around the element corresponding to that frequency band. Discovery of this is a two-stage process:

1. Compute

$$k_i^{max} = \arg\max_k \{A_i(k)\} \quad (6)$$

which is the location at which the i^{th}-scale decomposition reaches its maximum value.

2. Find the left and right "shoulders" of the peak according to

$$k_1^i = \max\{k : k < k_i^{max} \text{ and } A_i(k) < \eta_i\} + 1$$
$$k_2^i = \min\{k : k > k_i^{max} \text{ and } A_i(k) < \eta_i\} - 1$$

For scale i a candidate signal band is thus that of frequencies between $2\pi k_1^i/N$ and $2\pi k_2^i/N$ rad./sec.

6. – Estimate the signal energy profile for each scale as

$$\hat{\mu}_{1,1}^i = \frac{1}{k_2^i - k_1^i + 1}\sum_{j=k_1^i}^{k_2^i} A_i(j) \quad (7)$$

7. – Compute the GLR for scale i as

$$T_G^i = \prod_{m=1}^{L}\prod_{j=1}^{N}\frac{1}{\beta_j^i} e^{X_{jm}(1-1/\beta_j^i)} \quad (8)$$

or equivalently

$$T_g^i = \left[\sum_{m=1}^{L}\sum_{j=k_1^i}^{k_2^i} X_{jm}\left(1 - 1/\hat{\mu}_{1,1}^i\right)\right] - L(k_2^i - k_1^i + 1)\ln\left(\hat{\mu}_{1,1}^i\right) \quad (9)$$

8. – Find the overall GLR by maximizing over scales. That is,

$$T_G = \max_i \{T_G^i\} \quad (10)$$

is the overall test statistic.

The above procedure is quite ad hoc. But its computation is relatively light, and it works very well and robustly, both for narrowband and for broadband signals, and down to very low SNR values, as shown from figures 2 and figure 3. Since we have some interest

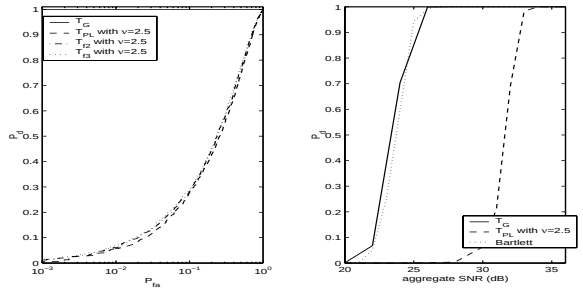

Fig. 2. Detection performance of our wavelet-based GLR detector for a signal with frequency band $[0.2, 0.2033]$. We set $N = 4096$ and $L = 100$. Here T_G represents our wavelet-based GLR scheme, T_{PL} for the power-law detectors, T_{f2} and T_{f3} for the power-law detectors combining 2 and 3 contiguous FFT bins respectively, and the Bartlett procedure is from [5]. In the left figure, the aggregate $SNR = 400$ is chosen to obtain the ROC curve. In the right figure, P_{fa} is given as 10^{-4}.

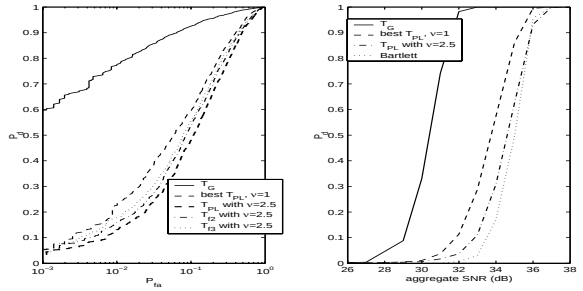

Fig. 3. Detection performance of our wavelet-based GLR detector for a signal with frequency band $[0.3, 0.4]$. (Left: aggregate $SNR = 1000$; Right: $P_{fa} = 10^{-4}$. Please note that (in this figure and others) the per-sample SNR is the given aggregate SNR minus $56dB$ – that is, the pictured aggregate SNR of $30dB$ is actually $-26dB$ per time-domain datum.

in signals with quite narrow bandwidth, we compare in this case the performance of our scheme to the Bartlett method (favored in [5] for the detection of a single tone in white Gaussian noise). In the first and most-narrowband case of figure 2 to which the Bartlett approach is "tuned" the performances are essentially identical; as the bandwidth increases in figure 3, the Bartlett scheme performs increasingly poorly.

3. EXTENSIONS

3.1. Extension to Signals with Multiple Bands

We can relax our assumptions such that the number of signal-occupied frequency bands is known to be $M > 1$, and use $[k_1(p), k_2(p)]$ to indicate the location of the p^{th} band with energy level $\mu_{1,p}$. A wavelet-based procedure as in section 2.2 is taken to estimate the parameters. The only substantive difference is that in step 7 we must compute

$$T_g^i = \sum_{p=1}^{M} \left[\sum_{m=1}^{L} \sum_{j=k_1^i(p)}^{k_2^i(p)} X_{jm} \left(1 - 1/\mu_{1,p}^i\right) \right] - \sum_{p=1}^{M} \left[L(k_2^i(p) - k_1^i(p) + 1) \ln\left(\hat{\mu}_{1,p}^i\right) \right] \quad (11)$$

The performance is illustrated and compared to the power-law detectors in figure 4. Further, the robustness with respect to an incorrect selection of M is studied and the loss is minor [4].

3.2. Extension to CFAR Operation for Nonwhite Data

The goal here is to detect a long-duration narrowband signal buried in colored noise with unknown but stationary spectrum. (The simpler case that the spectrum is known up to a scale constant is treated in [4], also.) We record the data as $\mathbf{X} = \{X_1, X_2, ..., X_{L^{norm}}, ..., X_L\}$, where X_{ji}'s are assumed independent and the first L^{norm} vectors are known to be noise-only.

We define the normalized observations as

$$z_j = \frac{\frac{1}{L - L^{norm}} \sum_{m=L^{norm}+1}^{L} X_{jm}}{\frac{1}{L^{norm}} \sum_{m=1}^{L^{norm}} X_{jm}} \quad (12)$$

for $j = 1, ..., N$. Here $\{z_j\}$ serves as the coarsely estimate $\{\beta_j^{uML}\}$. A procedure parallel to that in section 2.2 is used to estimate the β's and to test – the only difference is in the seventh step. According to the new (F-distributed) model we have

$$T_g^i = L \left[\sum_{j=k_1^i}^{k_2^i} \left(log(1 + \frac{L - L^{norm}}{L^{norm}} z_j) - log(1 + \frac{L - L^{norm}}{L^{norm}} \frac{z_j}{\hat{\mu}_{1,1}^i}) \right) \right] - (L - L^{norm})(k_2^i - k_1^i + 1) log\left(\hat{\mu}_{1,1}^i\right) \quad (13)$$

The above procedure can be easily modified to accommodate multiple signal bands.

From [3] we introduce the comparable power-law statistics T_{cpl}, defined as $T_{cpl} = \sum_{j=1}^{N} z_j^{\nu}$, where ν is a real exponent. By taking advantage of assumed frequency contiguity, we also form the detectors T_{cf2} and T_{cf3}, which combine respectively 2 and 3 contiguous DFT bins. The detection performance of the new scheme is illustrated and compared to the best CFAR power-law detectors in figures 5 and 6, with different choices of relative frequency bandwidth and signal power.

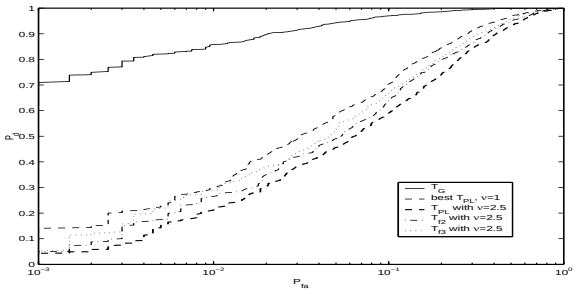

Fig. 4. Detection performance of our CFAR wavelet-based GLR detector for a signal with multiple frequency bands. Here the aggregate $SNR = 1200$, the band number $M = 3$.

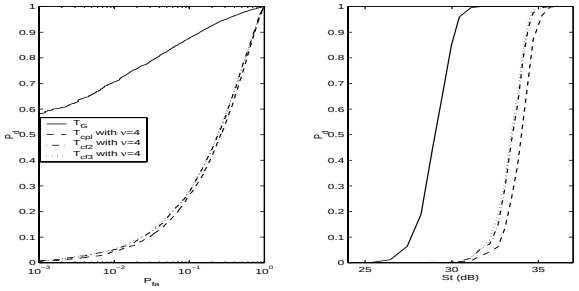

Fig. 5. Detection performance of the unwhitened CFAR version of the wavelet-based GLR detector for a signal with frequency band [0.3 0.31]. We set $N = 4096$,$L^{norm} = 30$, and $L = 90$.

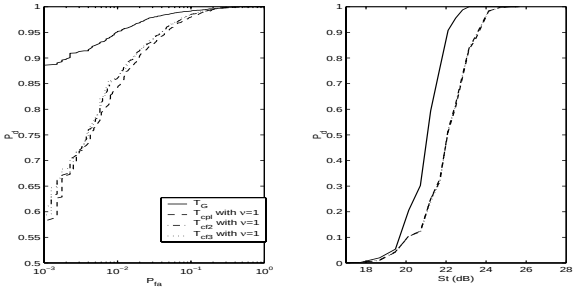

Fig. 6. Detection performance of the unwhitened CFAR version of the wavelet-based GLR detector for a signal with frequency band [0.2 0.5].

4. SUMMARY

In this paper we have sought a detector for a signal that is long, weak and narrowband. The scheme stages include magnitude-square discrete Fourier transformation, a multiresolution decomposition in the frequency domain with associated interpolation to preserve length, a peak-/band-picking routine at each scale, and formation of a GLR statistic. The scheme is admittedly ad hoc; however, its performance is good, and its computational load is comparable to that of the original DFT-step alone.

The procedure is flexible enough to admit a simple generalization to CFAR operation in the sense that, although a white background is assumed, its level may be unknown. There is little loss (less than $1dB$) from this generalization. A further generalization to the multiple "bands" of signal energy, is also explored. It is discovered that not only is the procedure straightforward and numerically-light, but also that there is little loss in over-estimating the number of bands. We additionally present a version of the detector that performs self-normalization on a frequency-by-frequency basis. (It naturally requires a stationary background noise process in order to do this.) The performance of this new scheme is, as above, remarkably good, and this may be considered a "plug-in" solution for the detection of band-constrained signals.

5. REFERENCES

[1] A. Nuttall, "Detection Performance of Power-Law Processors for Random Signals of Unknown Location, Structure, Extent, and Strength", NUWC-NPT Technical Report 10,751, September 1994.

[2] G. Strang and T. Nguyen, "Wavelet and Filter Banks", Wellesley-Cambridge Press, Wellesley, MA, 1996.

[3] Z. Wang and P. Willett, "All-Purpose and Plug-In Power-Law Detectors for Transient Signals", submitted to IEEE Transactions on Signal Processing, Aug., 2000.

[4] Z. Wang, P. Willett and R. Streit, "Detection of Long-Duration Narrowband Processes", submitted to IEEE Transactions on Aerospace and Electronic Systems, November 2000.

[5] H. So, Y. Chan, O. Ma and P. Ching, "Comparison of Various Periodograms for Sinusoid Detection and Frequency Estimation", IEEE Transactions on Aerospace and Electronic Systems, Vol. 35, No. 3, pp. 945-950, July 1999.